Soil and atmospheric dryness controls on fluorescence yield over global terrestrial ecosystems

S. De Cannière[1,2], M. Baur[3], D. Chaparro[4], T. Jagdhuber[4,5], F. Jonard[2,6]

[1]:Earth and Life Institute, Université catholique de Louvain, Louvain la Neuve, Belgium
[2]: Agrosphäre (IBG-3), Institute of Bio- and Geoscience, Forschungszentrum Jülich, Germany
[3]: Department of Geography, University of Cambridge, United Kingdom
[4]: Microwaves and Radar Institute, German Aerospace Agency (DLR), Wessling, Germany
[5]: Faculty of applied computer science: Institute of Geography, Augsburg University, Germany
[6]: Earth Observation and Ecosystem Modelling Laboratory, SPHERES research unit, Liège University, Belgium

Introduction

Sun-induced chlorophyll fluorescence is a promising drought stress indicator given its sensitivity to photosynthesis. Since photosynthesis is controlled by the stomatal opening it is expected that factors that affect stomatal dynamics have a downstream effect on the SIF emission. This research explores the effect of environmental variables and of plant physiological traits on fluorescence yield φ_F and compares these dynamics with expected dynamics in canopy conductance Gs. The environmental controls evaluated here are soil moisture (SM) and vapour pressure deficit (VPD), while the ecosystem isohydricty provided information on the on the ecosystem.

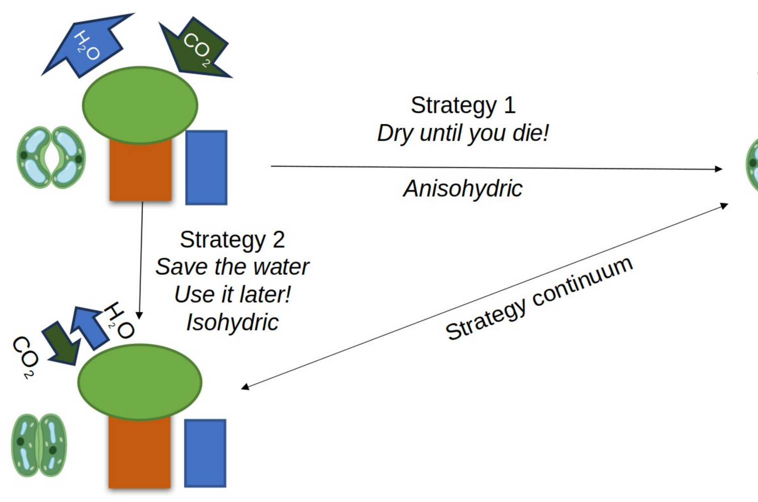

Figure 1: illustration of iso- and anisohydric strategies

Methodology

Sun-induced chlorophyll fluorescence (SIF) was taken from the TROPOMI-based TROPOSIF product (Guanter et al., 2021). Based on SIF, the fluorescence yield was retrieved by normalizing the SIF with NIRvP (=NIR_{rad} x NDVI), the latter accounting for variations in irradiation and for canopy structure dynamics. The environmental conditions of SM and VPD were retrieved from the Soil Moisture Active Passive (SMAP) and Atmospheric Infrared Sounder (AIRS), respectively. All data were re-projected to a 9 km EASE2 grid. The isohydricity data came from Konings & Gentine (2017), and provide an estimate of the strictness of the stomatal

The control of VPD and SM on φ_F was evaluated by means of phase spaces. In a phase space, the averages the φ_F over a specific set of SM-VPD conditions. In a first instance, the entire universe of φ_F observations is used to generate a general phase space. In a second instance, a sub-set of pixels is selected based on their ecosystem isohydricity.

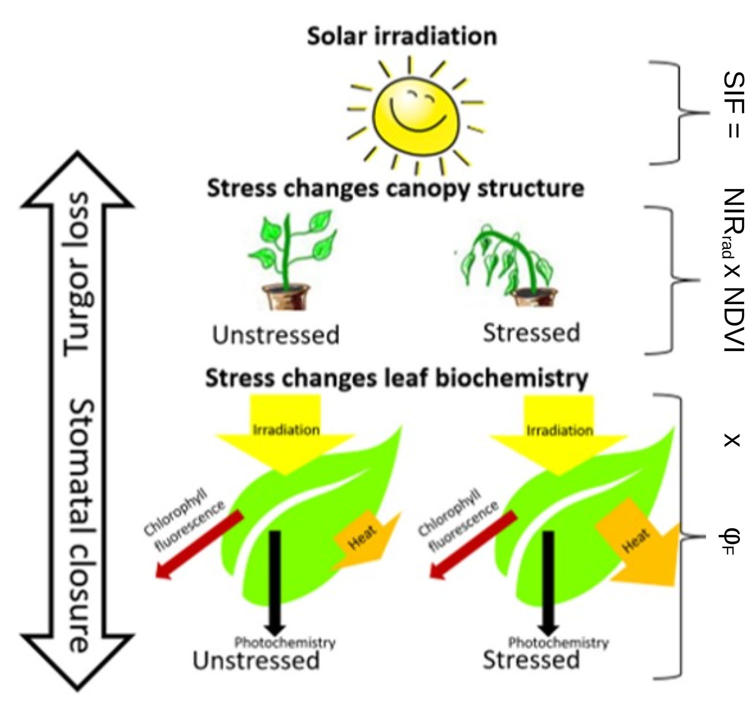

Figure 2: decomposition of the SIF signal to extract the physiological component from it

Behaviour φ_F before and after First 2019 European Heatwave

The effect of a heatwave, and thus of atmospheric dryness is made tangible by mapping the φ_F value over Western Europe before and after the First 2019 European Heatwave. Over almost the whole of Western Europe, the φ_F value decreased as a result of the heatwave.

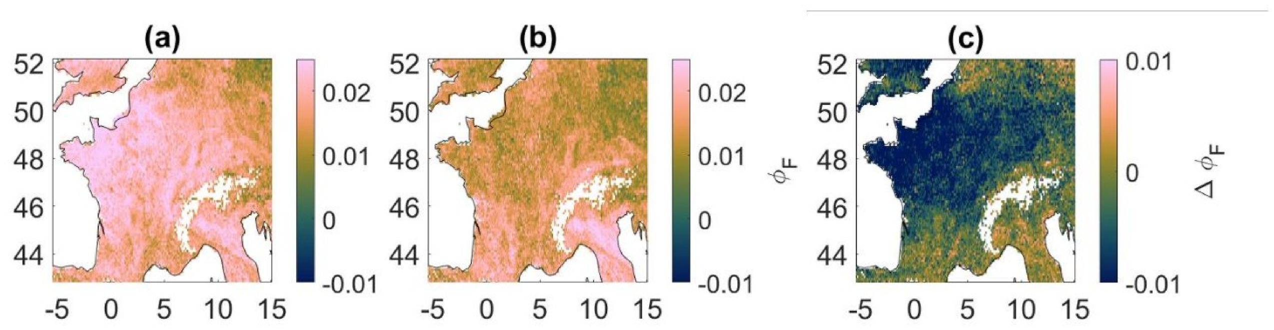

Figure 3: (a) Spatial overview of the average φ_F for June 1st -June 11th (b) Spatial overview of the average φ_F for June 25th -July 5th , the 2019 European heatwave; (c) difference in φ_F between Figures (a) and (b).

Global controls of soil moisture and vapour pressure deficit on φ_F

Figure 4a shows the phase space that considers the entire universe of TROPOMI φ_F measurements taken in 2019 and 2020. The φ_F data are averaged along their corresponding SM and VPD measurements. From these observations, a pattern emerges in which the φ_F maximizes when VPD is around 2.5 kPa, and SM is around 0.2. Figure 4b illustrates that the VPD dominates the φ_F emission for the lower VPD ranges. This is likely a combination of a irradiation and a temperature effect.

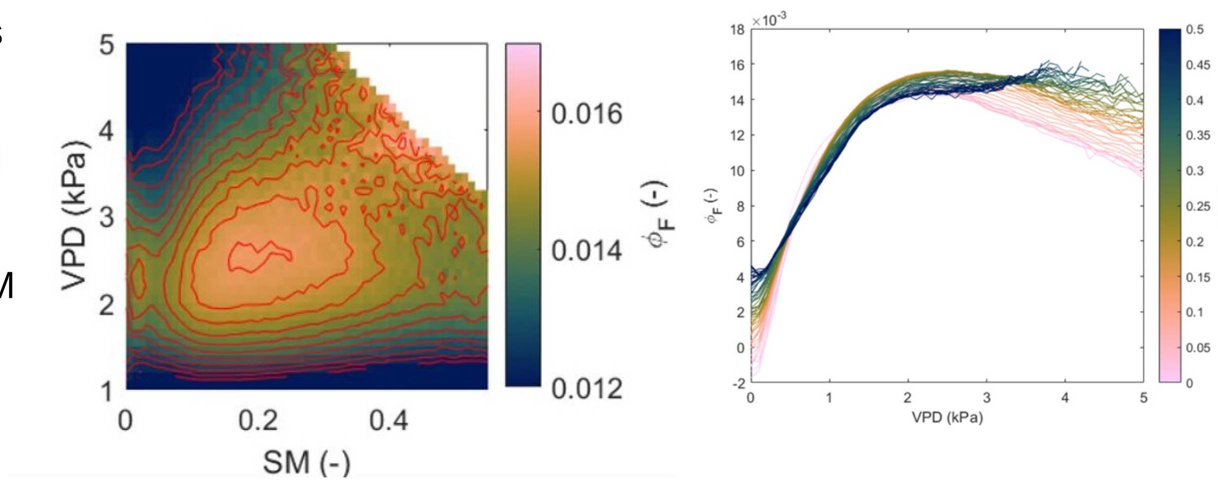

Figure 4: (a) global phase space of TROPOMI φ_f values (b) spaghettiplot showing the average φ_f value for each pixel from the phase space in figure 4a

Spatiotemporal comparison of φ_F and Gs dynamics

The VPD and SM data were put in the Wankmüller et al. (2021) plant hydraulics model, to caclculate Gs and the pixel-based Pearson's correlation coefficient between Gs and φ_F is calculated over the African continent. Some water-controlled regions show a high positive correlation coefficient (Figure 5).

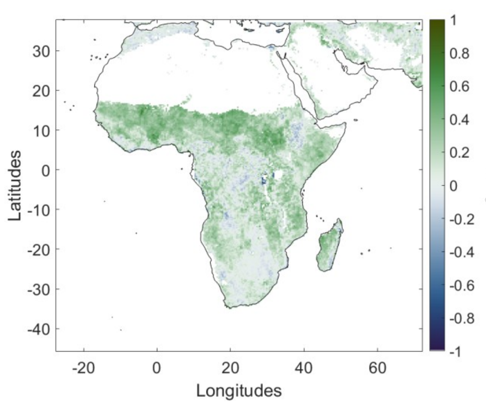

Figure 5: Map of pixel-based Pearson's correlation coefficient over Africa between φ_F and Gs for the years 2019-2020 .

Comparison of φ_F and Gs dynamics in a phase space

Figure 6 shows the φ_F averaged for the specific SM-VPD combinations, in function of their corresponding Gs value. The emerging pattern is a hyperbolic relationship, in which φ_F maximizes on a plateau in the high Gs-region, and with φ_F. The φ_F decreases dramatically when Gs < mmol $m^{-2}s^{-1}$. Low VPD allows for combinations in which φ_F is high while Gs is low.

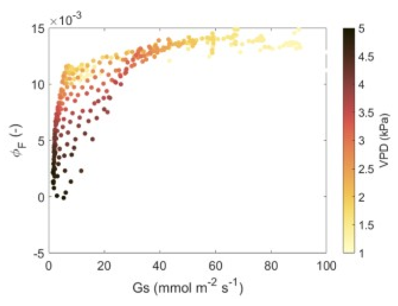

Figure 6: Map of pixel-based Pearson's correlation coefficient over Africa between φ_F and Gs for the years 2019-2020 .

Ecosystem isohydricity modulates VPD and SM control on φ_F

Figure 7 the trajectories of φ_F along the VPD axis for different SM and ecosystem isohydricity values. The most anisohydric category showed (I) the highest φ_F values and (II) the lowest sensitivity to SM and VPD compared to the more isohydric classes. The VPD-dominance for the region VPD < 1 kPa persisted for all isohydricity classes. Remarkably, the more isohydric classes show a higher φ_F value for the region VPD < 1 kPa compared to the their more anisohydric counterparts.

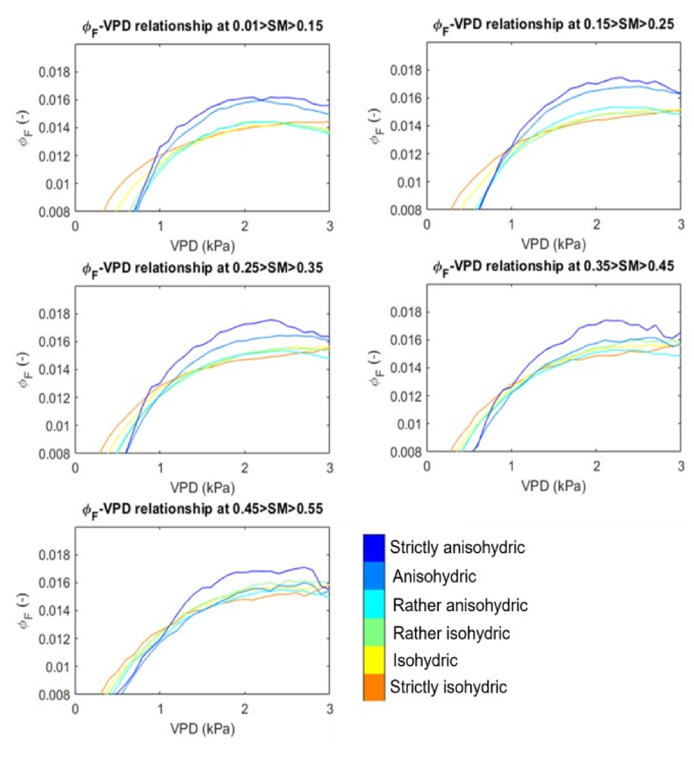

Figure 7: spaghettiplots of φ_F-VPD relationship for the average φ_f over eacht SM-VPD combination , stratified along isohydricities

Discussion and conclusion

The environmental variables VPD and SM drive φ_F variability. Consequently, φ_F shows an optimal zone for photosynthesis (m^3/m^3 < SM < 0.3 m^3/m^3 and 1.5 kPa < VPD < 2.5 kPa), in which φ_F is maximal. Also, φ_F is regulated only by VPD for low VPD values (<2.5 kPa), and coregulated by both VPD and SM for higher VPD values (>2.5 kPa). Results show that lower SM and/or higher VPD may lead to lowered stomatal conductance, lowering the φ_F. The case that large-scale φ_F is driven by stomatal dynamics is strengthened by the sensitivity of φ_F to isohydricity, since looser stomatal regulation was expected to lead to a weaker connection between φ_F on one hand and to SM-VPD on the other. The relationship between Gs and φ_F shows a hyperbolic shape, showing a resemblance to leaf-scale relationships between φ_F and Gs.

References

Guanter, L., Bacour, C., Schneider, A., Aben, I., Van Kempen, T.A., Maignan, F., Retscher, C., Köhler, P., Frankenberg, C., Joiner, J., Zhang, Y., 2021. The TROPOSIF global sun-induced fluorescence dataset from the Sentinel-5P TROPOMI mission. Earth System Science Data 13, 5423–5440. doi:10.5194/essd-13-5423-2021

Konings, A.G., Gentine, P., 2017. Global variations in ecosystem-scale isohydricity. Global Change Biology 23, 891–905. doi:10.1111/gcb.13389.

Wankmüller, F.J.P., Carminati, A., 2021. Stomatal regulation prevents plants from critical water potentials during drought: Result of a model linking soil-plant hydraulics to abscisic acid dynamics. Ecohydrology , 1–15doi:10.1002/eco.2386.